Available online at www.sciencedirect.com
SCIENCE DIRECT®
Journal of Sound and Vibration 267 (2003) 1127–1141
JOURNAL OF SOUND AND VIBRATION
www.elsevier.com/locate/jsvi

Resonance characteristics of high-speed trains passing simply supported bridges

S.H. Ju*, H.T. Lin

Department of Civil Engineering, National Cheng-Kung University, 1 Ta-Hsueh Road, Tainan 70101, Taiwan, ROC

Received 31 January 2002; accepted 30 October 2002

Abstract

This paper investigates the resonant characteristics of three-dimensional bridges when high-speed trains pass them. Multi-span bridges with high piers and simply supported beams were used in the dynamic finite element analysis. The dominated train frequencies proposed in this study can be clearly seen from the finite element result. To avoid resonance, the dominated train frequencies and the bridge natural frequencies should be as different as possible, especially for the first dominated train frequency and the first bridge natural frequency in each direction. If the two first frequencies are similar, the bridge resonance can be serious. This study also indicates that a suitable axial stiffness between two simple beams can reduce vibrations at a near-resonance condition. The axial stiffness of the continuous railway and the friction of the bearing plate should be enough to obtain this axial stiffness.

1. Introduction

Investigating the dynamic behavior of structures or bridges caused by the passing vehicles or trains has been an important subject of research since the 19th century. In early studies, moving vehicles travelling across a bridge were usually modelled as a series of moving loads or rolling masses. During the past several years, substantial theoretical and experimental research on the dynamic response of bridges has been carried out. More accurate models that consider the various dynamic characteristics of vehicles have been implemented in the study of vehicle–bridge interactions. The moving vehicle can be modelled as a one-foot dynamic system having two degrees of freedom [1,2]. More reasonable or complex multi-axle vehicles have been employed in the dynamic analysis of various types of bridges. Li and Su [3] researched the resonant vibration

*Corresponding author. Tel.: +886-6-2757575; fax: +886-6-2358542.
E-mail address: juju@mail.ncku.edu.tw (S.H. Ju).

0022-460X/03/$ - see front matter © 2002 Elsevier Science Ltd. All rights reserved.
doi:10.1016/S0022-460X(02)01463-3

for a simply supported girder bridge under high-speed trains. In their study, the vehicle idealized as a model of a rigid body and four wheel–axle sets, with two degrees of freedom of the vertical correspond to bounce and pitch motion. Au et al. [4] used a four-axle (10 degrees of freedom) train model to study the impact effects on a cable-stayed bridge under railway train loading. Xia et al. [5] adopted a four-axle (27 degrees of freedom) vehicle model in the dynamic analysis of a long suspension bridge with a 1377 m main span. Zhang et al. [6] developed the three-dimensional model for train carriages and in dynamic analysis of the vehicle–bridge interaction. Recently, the vehicle–bridge interaction element has been developed for modelling the vehicle–bridge interaction in dynamic analysis of bridges under high-speed trains or vehicles. Yang et al. [7] applied the dynamic condensation method to analyze the impact effects of simply supported beams and three-span continuous beams subjected to a moving five-axle truck. Yang and Wu [8] presented a suitable numerical model for handling both the vehicle and bridge response that are of particular interest in high-speed railway. Ju [9] used the three-dimensional FEM to simulate the soil vibrations due to the moving high-speed train across bridges. He first analyzed the bridge system passed by a train. Then, the calculated pier forces and moments were applied to a pile cap in order to simulate the wave propagation in soil.

Since bridges often contain piers to support the loading from bridge girders, to study the bridge resonance, the pier effect cannot be ignored. However, few researches performed the bridge resonance analysis including bridge piers. This paper studies the resonant vibration characteristics of the three-dimensional vehicle–bridge system when high-speed trains pass bridges. Multi-span bridges with high piers and simply supported beams were used in the dynamic finite element analysis. The resonance characteristics of the simply supported bridge including high piers under high-speed trainloads were investigated.

2. Dominated frequency of moving trains

When a series of train sections passes bridges, train wheel loads will act on the bridge periodically. The period means the time during which the forward part of the train enters a bridge until the next forward part of the train does so. Thus, for the investigation of the resonant vibration of high-speed trains passing bridges, the dominated frequencies of moving trains should be known first. To evaluate the dominated frequencies of the train loads, the wheel loading of the moving train passing a point is assumed to be a periodic function $p(t)$ as follows:

$$P(t) = P_{wheel}[\delta(t - t_1) + \delta(t - t_2) + \delta(t - t_3) + \delta(t - t_4)], \tag{1}$$

where we assume that each train compartment has four pairs of wheels, P_{wheel} is the load of a pair of wheels, ($\delta(t - t_i)$, $i = 1-4$) is the unit impulse function at t_i and $t_i = s_i/V$, where V is the train velocity and s_i is the distance between the ith wheel and the beginning of the compartment. This $P(t)$ has a frequency of V/L (or period of L/V) where L is the distance between two compartment centers. The Fourier exponential series is applied to Eq. (1) to obtain

$$F(t) = \sum_{n=-\infty}^{\infty} C_n e^{in\omega t}, \tag{2}$$

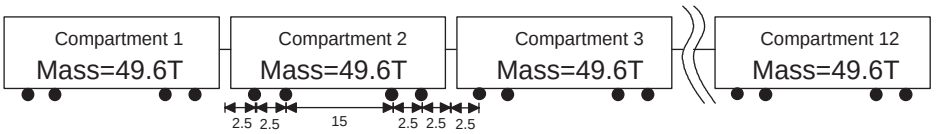

Fig. 1. Mass and dimensions of the modified SKS-700 high-speed train.

$$C_n = \frac{1}{T}\int_0^T F(t)\mathrm{e}^{-\mathrm{i}n\omega t}\,\mathrm{d}t = \frac{1}{T}(\mathrm{e}^{-\mathrm{i}n\omega t_1} + \mathrm{e}^{-\mathrm{i}n\omega t_2} + \mathrm{e}^{-\mathrm{i}n\omega t_3} + \mathrm{e}^{-\mathrm{i}n\omega t_4}). \tag{3}$$

Thus, the dominated frequencies f_n of these wheel loads and their influence factors R are

$$f_n = nV/L, \tag{4}$$

$$R = |C_n|, \tag{5}$$

where n $(=1, 2, 3, \ldots)$ is a positive integer. Eq. (4) indicates that f_n is dependent on the train velocity and the compartment length but independent of the wheel arrangement. The wheel arrangement will affect the magnitude of R. To consider the characteristics of the structural dynamics, the low frequencies, especially for the first frequency ($f_1 = V/L$), are often dominated. To avoid the resonance of bridges and trains, the first frequency (V/L) of the wheel loading and the first bridge natural frequencies should be as different as possible.

For the high-speed train of Japan SKS-700 with a vehicle length of 25 m (Fig. 1), when the speed of the train is fixed at $V = 300\,\mathrm{km/h} = 83.33\,\mathrm{m/s}$, the first frequency is $f_1 = (83.33\,\mathrm{m/s})/(25\,\mathrm{m}) = 3.33\,\mathrm{Hz}$. Similarly, the second and the third frequencies are $f_2 = 6.66\,\mathrm{Hz}$ and $f_3 = 10\,\mathrm{Hz}$.

3. Finite element model of vehicles

The high-speed train was simulated as several moving wheel elements containing a mass M_v, damping c_v and stiffness k_v as shown in Fig. 2. The element includes a wheel node and several target nodes. When the present wheel position is known, the two target nodes in which the wheel is located between them can be found. If the two target nodes and the wheel node are set to be nodes 1, 3 and 2, respectively, the mass, damping, and stiffness of the three-node element can be calculated as below using a similar procedure as in Ref. [10]:

$$\begin{aligned}[S] &= \begin{bmatrix} 0 & s_n \\ 1 & 0 \\ 0 & s_m \end{bmatrix} \begin{bmatrix} S_1 & S_2 \\ S_2 & S_3 \end{bmatrix} \begin{bmatrix} 0 & 1 & 0 \\ s_n & 0 & s_m \end{bmatrix} \\ &= \begin{bmatrix} s_n^2 S_3 & s_n S_2 & s_n s_m S_3 \\ s_n S_2 & S_1 & s_m S_2 \\ s_n s_m S_3 & s_m S_2 & s_m^2 S_3 \end{bmatrix}, \end{aligned} \tag{6}$$

where $\mathrm{s_n} = L_{2-3}/L_{1-3}$, L_{2-3} is the length between nodes 2 and 3, L_{1-3} is the length between nodes 1 and 3, $s_m = 1 - s_n$ and S_1, S_2 and S_3 are the components of the mass, damping or stiffness

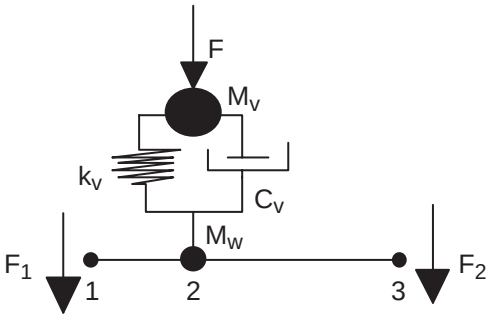

Fig. 2. Moving wheel element.

matrix of the vehicle wheel. For the mass, $S_1 = M_v$, $S_2 = 0$ and $S_3 = M_w$ (M_w is small and can be set to zero), for the damping $S_1 = S_3 = c_v$ and $S_2 = -c_v$ and for the stiffness $S_1 = S_3 = k_v$ and $S_2 = -k_v$, in which M_v, M_w, c_v and k_v are the train mass, wheel mass, damping and stiffness shown in Fig. 2. The direction of the three-node matrix can be one of the three global translations or the three global rotations. Since the wheel load F shown in Fig. 2 is equilibrium on the system, this load F on node 2 should be transformed into nodes 1 and 3 to obtain the force vector $\{f\}$ as follows:

$$\{f\} = \begin{Bmatrix} F_1 \\ 0 \\ F_2 \end{Bmatrix} = \begin{Bmatrix} s_n F \\ 0 \\ s_m F \end{Bmatrix}. \tag{7}$$

The rail irregularity in the vertical and transverse directions can be modelled as

$$D_Z(X) = \frac{a_Z}{2} \sin(2\pi X / L_Z), \tag{8}$$

$$D_Y(X) = \frac{a_Y}{2} \sin(2\pi X / L_Y), \tag{9}$$

where a_Z is the amplitude of the rail irregularity in the vertical direction, a_Y is that in the transverse direction, L_Z is the wavelength of the rail irregularity in the vertical direction and L_Y is that in the transverse direction. From measurements, the irregular amplitude is often between 0.5 and 2.5 mm, and the irregular wavelength is often between 100 and 600 mm. This irregular shape produces unbalanced forces at node 2 as shown in Eq. (10). These forces should be added to the internal forces of node 2 to ensure the balance of the internal, inertia, damping and external forces at this node:

$$\begin{Bmatrix} f_Z \\ f_Y \end{Bmatrix} = \begin{Bmatrix} -k_v D_Z - c_v \dot{D}_Z \\ -k_v D_Y - c_v \dot{D}_Y \end{Bmatrix}. \tag{10}$$

To verify the moving wheel element, a rigid surface passed by a wheel was analyzed. The rigid surface has an irregular shape according to Eqs. (8) and (9) with $a_Z = 0.01$ m, $a_Y = 0$ and

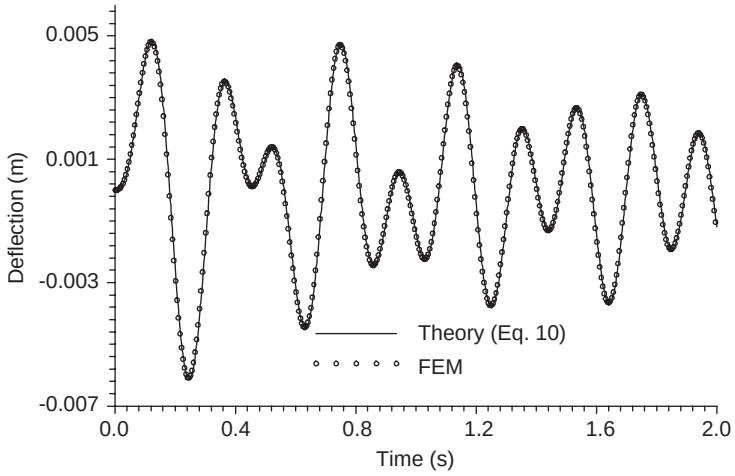

Fig. 3. Comparison between theoretical and FEM solutions for a rigid foundation with irregular vertical shape.

$L_Z = 10\,\text{m}$. The moving wheel has the following parameters: $k_v = 2\text{E}6\,\text{N/m}$, $M_v = 6000\,\text{kg}$, $M_w = 0$, $v = 50\,\text{m/s}$, $c_v = 1\text{E}4\,\text{N-s/m}$ and $\gamma = 2352\,\text{kg/m}$, where γ is the mass per unit length of the beam. The theoretical solution of this problem is

$$M_v\ddot{Z} + c_v\dot{Z} + k_vZ = c_v\dot{D}_Z + k_vD_Z. \tag{11}$$

The finite element model only contains three nodes, one wheel node and two target nodes. The comparison between finite element and theoretical results are shown in Fig. 3, which indicates an identical result.

To model the high-speed train, first define the target nodes passed by the train, and then model each train wheel as a moving wheel element with appropriate velocity, initial position, load, mass, damping and stiffness in global X, Y and Z directions. Thus, a direct integration method can be used to perform the finite element analysis. The advantage of this moving wheel element is that the formulation and use of the elements are simple. The disadvantage is that the mass, damping and stiffness matrices vary with wheel position, which produces a non-linear finite element analysis. This condition is not serious, since for a problem with large degrees of freedom, the efficient conjugate gradient method is often used to solve the matrix equation. At this time, the Newton–Raphson method that forms a new tangent stiffness at each iteration has been suggested as the best scheme.

4. Three-dimensional finite element analyses of bridges

In Fig. 4, a seven-bay bridge system modelled by three-dimensional beam elements is adopted in this study, where the X-axis is the railway direction, the Y-axis is perpendicular to the railway, and the negative Z-axis is the soil depth direction. The foundations including soils, piles

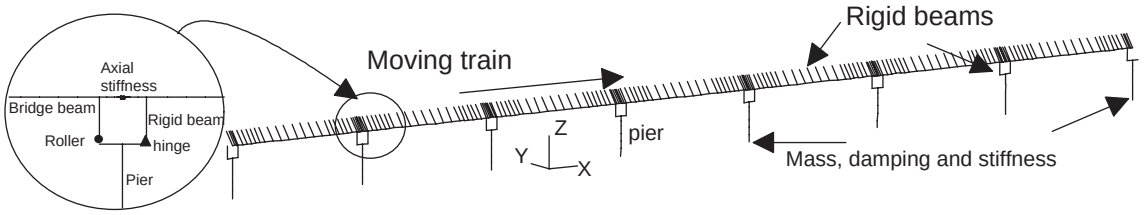

(a) Finite element model

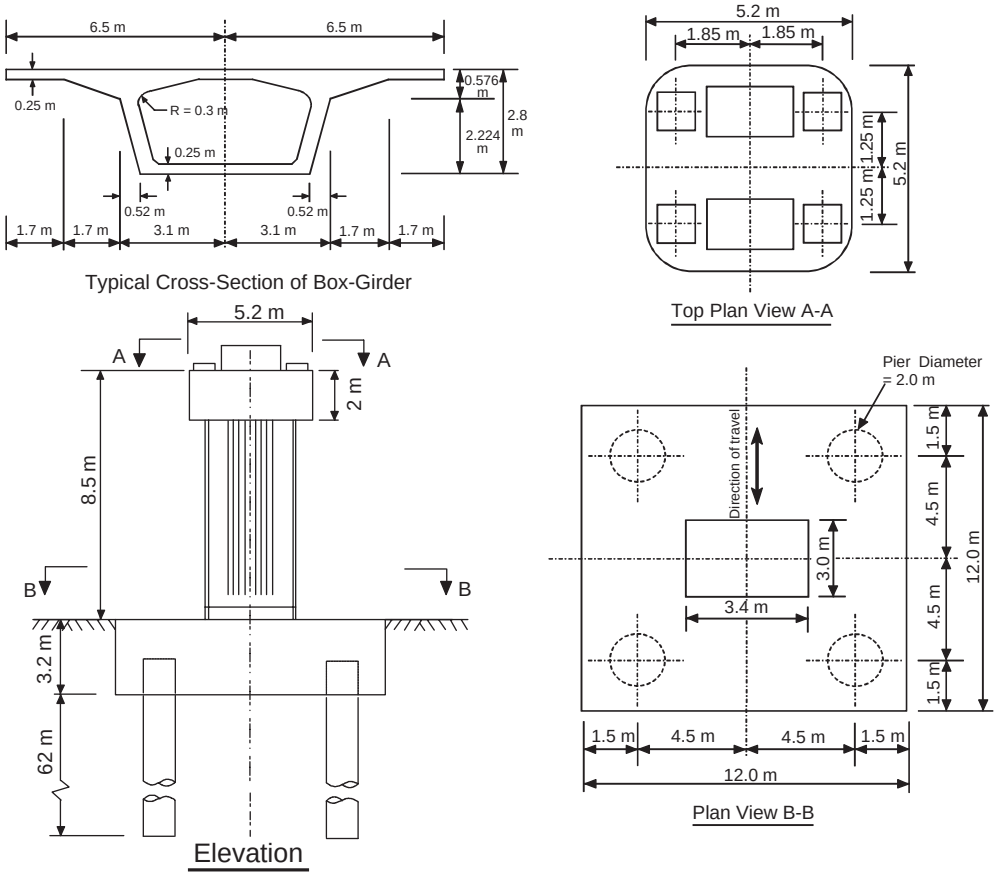

(b) bridge pier, piles and beam dimensions

Fig. 4. Finite element model and dimensions of the bridge.

and the pile cap were modelled using input stiffness, damping and mass matrices, which are calculated using the least-squares method from Ref. [9]. The three matrices at the loading frequency of 30 rad/s are shown in Eqs. (12)–(14), which are used in the following finite element analyses.

Foundation mass matrix:

$$[M] = \begin{bmatrix} 1.497\text{E}+3 & 0 & 0 & 0 & -1.140\text{E}+2 & 0 \\ 0 & 1.497\text{E}+3 & 0 & 1.140\text{E}+2 & 0 & 0 \\ 0 & 0 & 9.000\text{E}+2 & 0 & 0 & 0 \\ 0 & 1.140\text{E}+2 & 0 & 6.467\text{E}+3 & 0 & 0 \\ -1.140\text{E}+2 & 0 & 0 & 0 & 6.467\text{E}+3 & 0 \\ 0 & 0 & 0 & 0 & 0 & 3.255\text{E}+4 \end{bmatrix}. \quad (12)$$

Note: Units for translational and rotational mass values are ton and ton-m^2.

Foundation damping matrix:

$$[C] = \begin{bmatrix} 1.230\text{E}+5 & 0 & 0 & 0 & -1.285\text{E}+5 & 0 \\ 0 & 1.230\text{E}+5 & 0 & 1.285\text{E}+5 & 0 & 0 \\ 0 & 0 & 1.353\text{E}+5 & 0 & 0 & 0 \\ 0 & 1.285\text{E}+5 & 0 & 3.842\text{E}+5 & 0 & 0 \\ -1.285\text{E}+5 & 0 & 0 & 0 & 3.842\text{E}+5 & 0 \\ 0 & 0 & 0 & 0 & 0 & 1.141\text{E}+6 \end{bmatrix}. \quad (13)$$

Note: Units for translational and rotational damping values are kN-s/m and kN-s-m.

Foundation stiffness matrix:

$$[K] = \begin{bmatrix} 4.129\text{E}+6 & 0 & 0 & 0 & -4.680\text{E}+6 & 0 \\ 0 & 4.129\text{E}+6 & 0 & 4.680\text{E}+6 & 0 & 0 \\ 0 & 0 & 9.293\text{E}+6 & 0 & 0 & 0 \\ 0 & 4.680\text{E}+6 & 0 & 1.436\text{E}+8 & 0 & 0 \\ -4.680\text{E}+6 & 0 & 0 & 0 & 6.467\text{E}+3 & 0 \\ 0 & 0 & 0 & 0 & 0 & 1.825\text{E}+8 \end{bmatrix}. \quad (14)$$

Note: Units for translational and rotational stiffness values are kN/m and kN-m.

The simple bridge beam supported on the bearing plates is not on the pier center, so a rigid beam system shown in Fig. 4 was used to model this eccentricity. Moreover, because the distance between the railroad center and the pier center is 2.25 m, very rigid beam elements whose Young's modulus is 100 times as large as that of the concrete were arranged in the X direction shown in Fig. 4 to model this condition. The simply supported railroad bridges along the X-axis have a pier spacing of 30 m and pier height of 8.5 m. The Y-axis is perpendicular to the railroad bridge, and the Z-axis is the soil depth direction. The SKS-700 high-speed train passing the bridges was simulated using the non-linear Newmark direct integration method with the consistent mass scheme. The time step length was set to 0.0022 s, and totally 4000 time steps were used. The solution of each time step was converged within two Newton–Raphson iterations averagely. The two factors of Rayleigh damping ($[Damping] = \alpha[Mass] + \beta[Stiffness]$) α and β equal 0.458/s and 6.35E−4 s/m, respectively, which is approximate to the damping ratio of 3%. The train velocity was set from 50 to 600 km/h with an increment of 10 km/h, so there were 56 finite element analyses

Table 1
First-mode bridge natural frequencies in the three global directions

	X direction (railway direction)	Y direction	Z direction (vertical direction)
Natural frequency (Hz)	2.85	2.39	4.82

for a certain bridge structure. The spring stiffness and the damping of the SKS-700 two-wheel set are $k_X = k_Y = k_Z = 1800\,\text{kN/m}$, $c_Y = 0$ and $c_X = c_Z = 25\,\text{kN s/m}$, in which the subscripts X, Y and Z means the global directions shown in Fig. 4. The parameters of the rail irregularity were given as $a_Z = a_Y = 1.0\,\text{mm}$ and $L_Z = L_Y = 250\,\text{mm}$. The finite element result from this rail irregularity is about 2% different from those without the rail irregularity, which shows that the rail irregularity effect of the bridge used in this study is minor. Since this paper investigates the resonance effect, the model analysis was also performed to find the bridge natural frequencies. Table 1 shows the first-mode natural frequencies in the three global directions.

5. Finite element results and resonant characteristics

After 56 finite element analyses for a certain bridge structure were performed, the three element forces, X-shear, Y-shear and Z-axial forces, at the third pier bottom were transformed to the frequency domain using the fast Fourier transform (FFT) for each finite element analysis. Then, using the velocities and frequencies for the two horizontal axes and the force magnitudes for the vertical axis, one obtains a wire-frame figure. For example, Fig. 5a shows the time–history Z-axial forces at the pier bottom hanging with time from the finite element result. The averaged dead weight of 583 kN ($=49.6\,\text{t} \times 9.8\,\text{m/s}^2 \times 30\,\text{m}/25\,\text{m}$, where 49.6 t is the mass of a train compartment shown in Fig. 1, 30 m is the bridge length per simple beam span and 25 m is the compartment length) similar to the averaged Z-axial force in Fig. 5a indicates that the finite element result was reasonable. Then, we put the data of Fig. 5a into the FFT to find the Z-axial forces changing with frequencies, which are shown in Fig. 5b. Finally, assembling all this frequency-domain figures changing with train velocities, one obtained a wire-frame figure.

Fig. 5a shows that the train speed of 300 km/h will only generate a 0.25-Hz (period = 4 s measured from Fig. 5a) load from the dead weight. Since the first natural frequencies of the bridge in three global directions are much higher than this dead weight frequency in this study, resonance will not occur near the dead weight frequency. Moreover, the train dead weight produces a large coefficient of FFT at the zero frequency, which also causes various errors of the frequencies near zero. Thus, we did not show this low frequency in wire-frame figures, but showed the responses whose frequencies are higher than 2 Hz.

5.1. Vibration reduction by the railway longitudinal stiffness between simple beams

For simple beam bridges at piers, the beams in the axial direction are not continuous, but the rails across two simple beams are continuous; moreover, the roller bearing plates at the pier support have a frictional coefficient from 0.05 to 0.2, which can sustain the axial frictional force

from 300 to 1200 kN of the simple beam shown in Fig. 4. For strong earthquakes, this axial railway stiffness and the frictional force cannot produce a continuous effect, but under the moving train loading, they are definitely helpful to the longitudinal continuity of the simple beams. For example, without considering the axial stiffness of simple beams, the axial force transferred from the simple beam to the pier of the bridge system in Fig. 4 is from 50 to 400 kN, which is even smaller than the range of the frictional force. Thus, an axial stiffness of 1.23E6 kN/m was used to model the axial railway stiffness and the bearing friction in the finite element model. This stiffness is equivalent to a steel bar of 3.2-cm diameter connecting two simple beams. Fig. 6 shows the time–history X-shear forces at the third pier bottom changing with time from five finite element

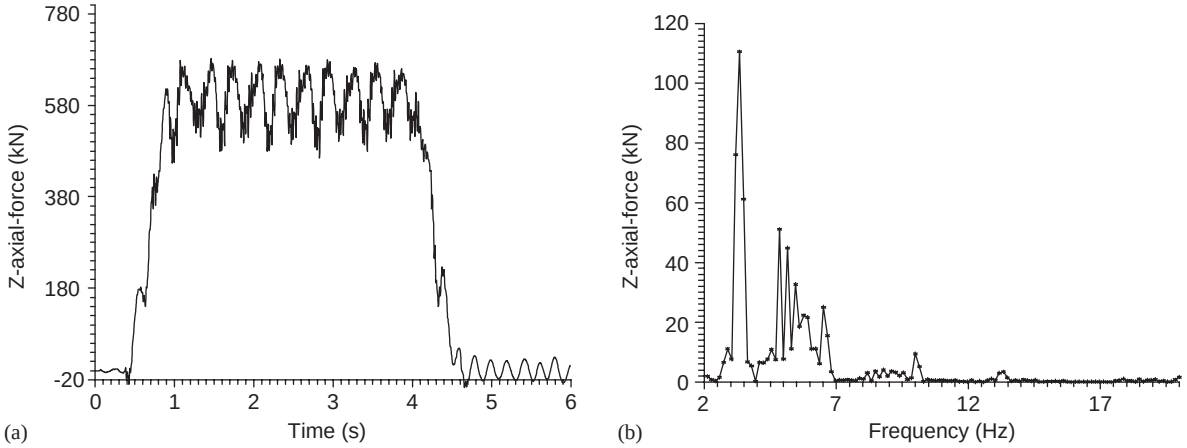

Fig. 5. Z-axial forces at the third pier bottom (a) changing with time and (b) changing with frequencies (train speed = 300 km/h).

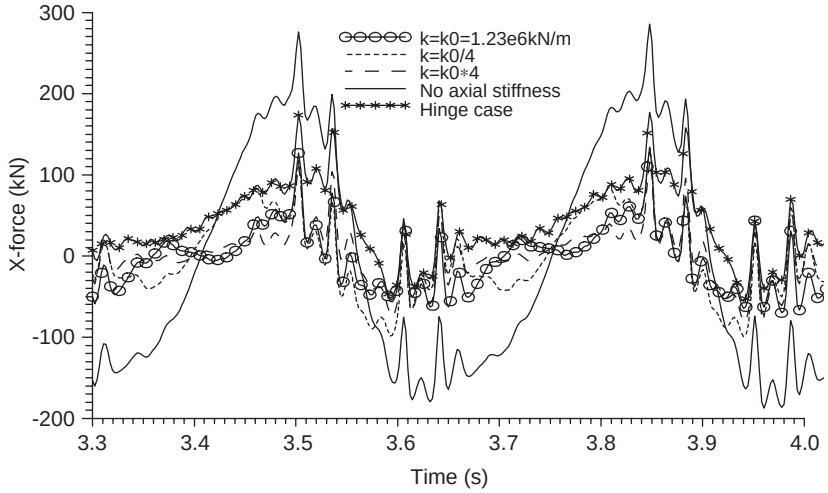

Fig. 6. X-shear forces at the third pier bottom changing with time for five cases with different axial stiffness between simple beams (train speed = 260 km/h) (time-domain results).

analyses with different axial stiffness (k) between simple beams, where the k of case 1 equals $k0 = 1.23E6\,kN/m$, the k of case 2 equals $k0/4$, the k of case 3 equals $k0 \times 4$, the k of case 4 equals zero and case 5 replaces simple beam rollers by hinges. The train velocity was set to 260 km/h which produces a near-resonance condition of the bridge and moving train in the X direction. This figure indicates that the X-shear forces of $k0$, $k0/4$, $k0 \times 4$ and hinge cases are similar, but they are much smaller than the X-shear forces of case 4 which do not have the axial stiffness between simple beams. This means that (1) a very small axial stiffness between simple beams can avoid resonance in the X direction and (2) the resonance reduction is not sensitive to the value of the axial stiffness. The bearing plate friction and the continuous rail can give equivalent axial stiffness that is enough to decrease bridge vibrations from moving vehicles.

Figs. 7 and 8 show the X-shear forces at the third pier bottom with and without the axial stiffness between two simple beams. Without the axial stiffness between simple beams, the X-vibration increases considerably near the frequency of 2.9 Hz at the train speed of 260 km/h (point A in Fig. 7). The reason is when the train runs with the speed of 260 km/h, the dominated frequency of the train loading is $V/L = 2.9$ Hz, which is very close to the bridge X direction natural frequency of 2.85 Hz shown in Table 1. At this time, the X direction resonance causes large horizontal vibrations. When the axial stiffness is arranged between simple beams, this restraint causes the X-vibrations of bridge piers moving together in a direction, and the separate vibrations of the pier are much smaller than those without the axial stiffness. Thus, the X-resonance effect will decrease significantly due to the equivalent axial stiffness for simple beams. The vibration patterns of the other two directions (Y and Z directions) change little for the cases with and without the axial stiffness. The wire-frame figures of Y and Z directions are shown in Figs. 9 and 10, respectively.

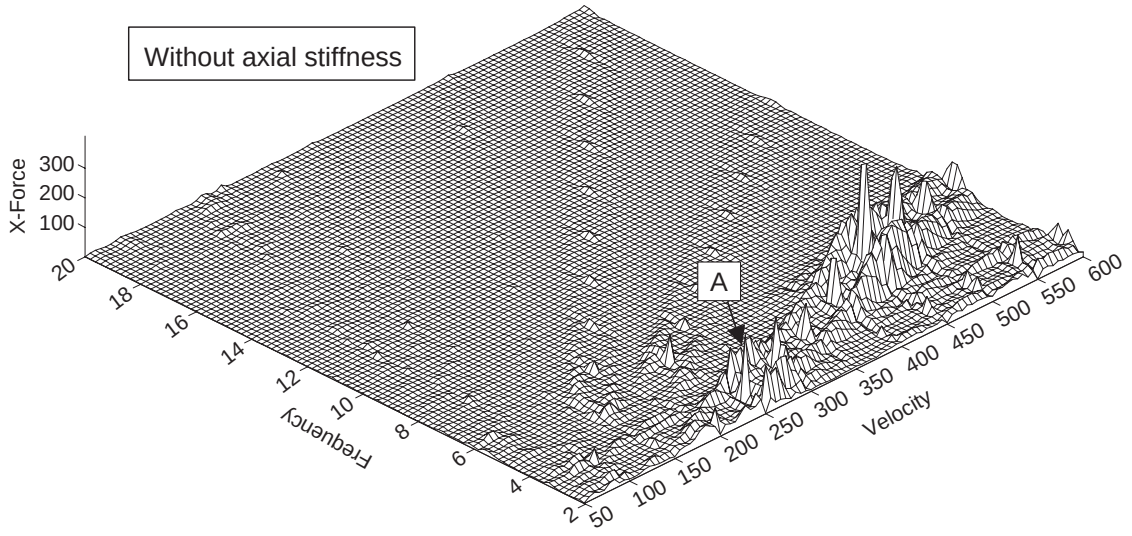

Fig. 7. Frequency-domain internal forces in the railway direction (X direction) at the third pier bottom changing with velocity (50–600 km/h). (The axial stiffness between simple beams is not considered.)

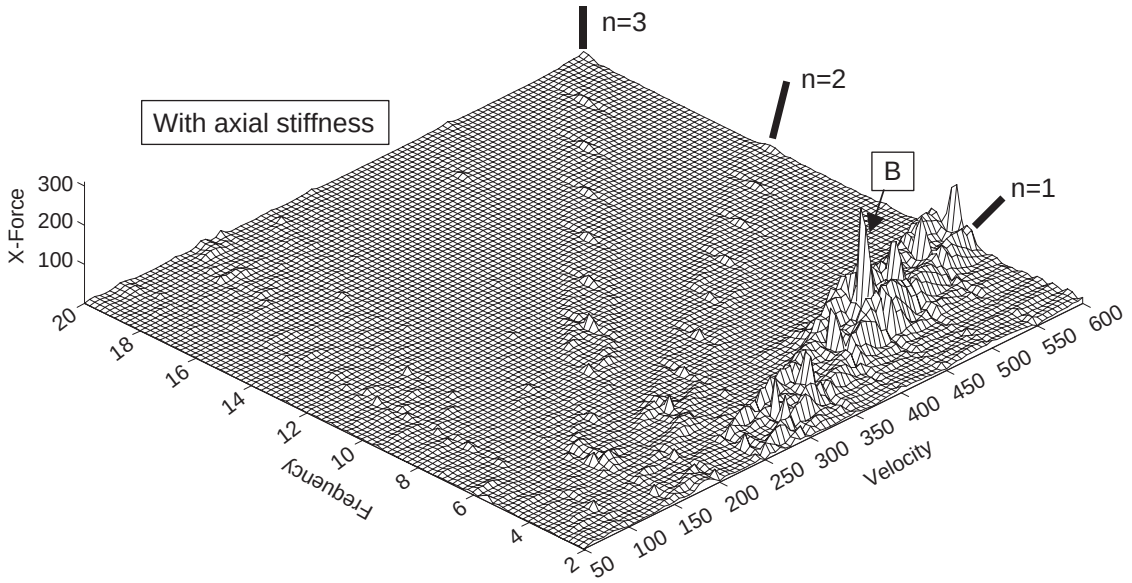

Fig. 8. Frequency-domain internal forces in the railway direction (X direction) at the third pier bottom changing with velocity (50–600 km/h). (The axial stiffness between simple beams is considered.)

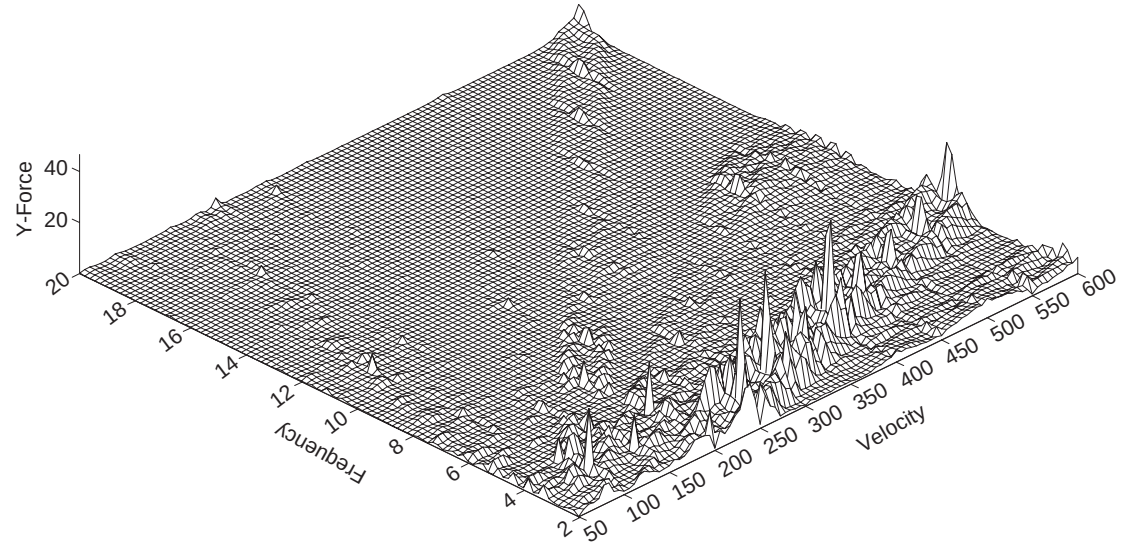

Fig. 9. Frequency-domain internal forces in the Y direction at the third pier bottom changing with velocity (50–600 km/h).

5.2. Three-direction resonant characteristics of simply supported bridges

The high-speed train passing simply supported bridges causes vibrations vertically. When the train-dominated frequencies approach the vertical natural frequencies, the resonance in the vertical direction occurs, which can be clearly seen at point C of Fig. 10, where the Z-force peak is

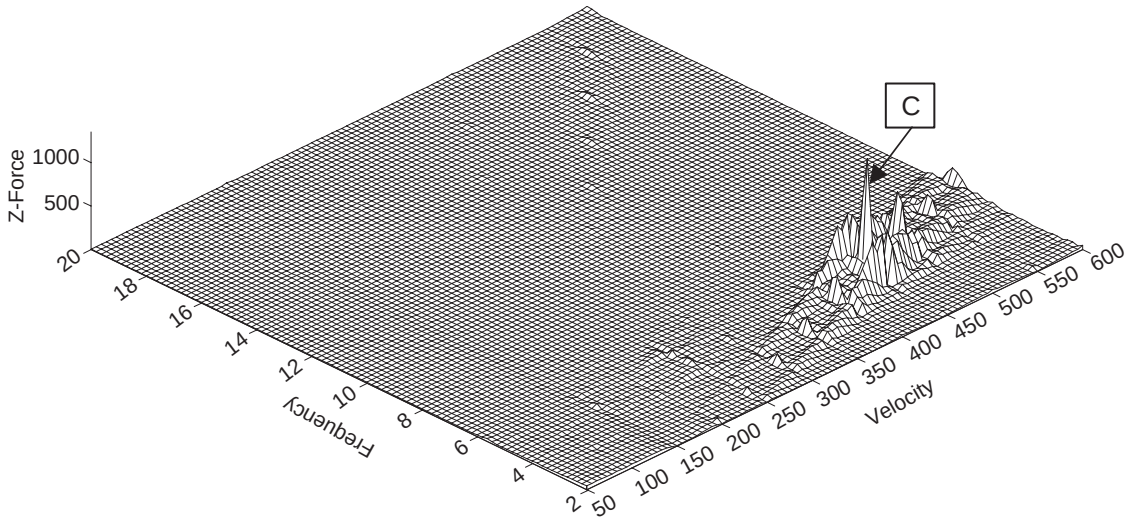

Fig. 10. Frequency-domain internal forces in the vertical direction (Z direction) at the third pier bottom changing with velocity (50–600 km/h).

located at the first train-dominated frequency ($V = 450$ km/h) and the first vertical natural frequency (4.8 Hz). The X-vibrations (in the railway direction) are caused from the eccentricity of simply supported beams on piers, and the vibration amplitude is proportional to the eccentricity. Thus, the resonance in the vertical direction also triggers large vibrations in the X direction, which can be found at point B of Fig. 8. According to the discussion of the previous section, the resonance is not obvious when the axial stiffness is modelled between simple beams. Therefore, the highest peak of the X-vibration pattern in Fig. 8 is produced from the vertical resonance. The Y-vibrations are produced from the eccentricity of the railway. The vibration pattern of Y direction is much smaller than those of X and Z directions. The reason is because the bridge mass is not eccentric, and the eccentric train mass is only one-tenth of the bridge beam mass. Moreover, the axial rotation of the simple beams on piers is continuous, which will reduce the resonance effect.

5.3. *Characteristics of the high-speed train-dominated frequencies*

The dominated frequencies of trains are nV/L discussed in Section 2. Since the compartment interval L is constant, the dominated frequency for a certain n is linearly proportional to the train velocity V. This condition can be validated using the finite element results shown in Fig. 8, in which the first dominated frequency ($n = 1$) is linearly proportional to the train velocity very obviously. The second and third dominated frequencies still have this linear relationship with train velocities even though the force magnitudes of the two dominated frequencies are much smaller than that of the first dominated frequency. The large vibration effect of the first dominated frequency is because the arrangement of the train wheels produces an obvious R in

Eq. (5); moreover, the lower frequency often causes larger structural vibrations. When the train wheels are re-arranged to equal space as shown in Fig. 11, the influence factors R for $n = 1$ and 3 are near zero. The finite element analyses of this wheel arrangement were performed. The results of X-vibrations are shown in Fig. 12, which indicates that the force magnitudes of the first dominated frequency are much smaller than those of the second dominated frequency. The force magnitudes of the third dominated frequency even approach zero. This finite element result exactly confirms the consequence of Eqs. (4) and (5). For complex three-dimensional bridges, to find a theoretical dynamic solution due to the high-speed train loading is considerably difficult. This study proposes the following easy method to check the resonance condition of bridges:

(1) First, the modal analysis of the bridge is performed to obtain the natural frequencies of the bridge. The finite element mesh should include the bridge superstructures, bridge piers and foundations. The modelling of the bridge foundations is usually difficult, so the equivalent mass, damping and stiffness matrices can be used to simulate bridge foundations.
(2) Structural natural frequencies, especially for the first natural frequency in each direction, should be as different as possible from the dominated frequencies of the train $f_n = nV/L$.

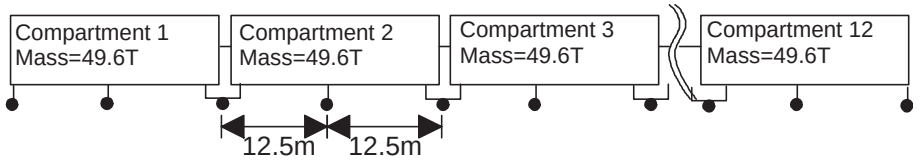

Fig. 11. Mass and dimensions of the equal-space-wheel high-speed train.

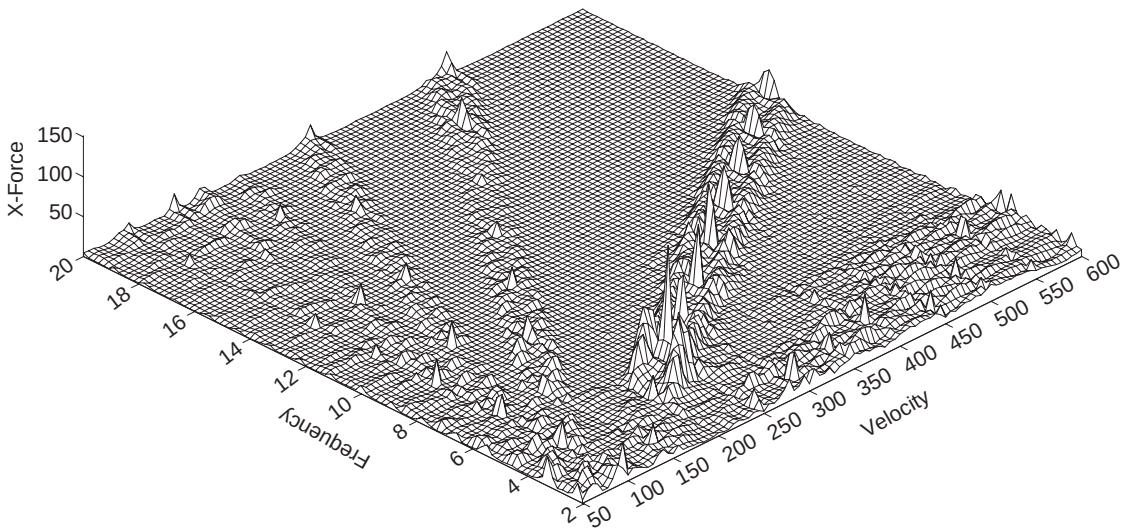

Fig. 12. Frequency-domain internal forces in the railway direction (X direction) at the third pier bottom changing with velocity (50–600 km/h). (The equal-space wheels are arranged in the train.)

(3) If the influence factor R of the first dominated frequency does not approach zero, the frequency $f_1 = V/L$ should be the most important one to produce bridge resonance. Only the uniform arrangement of more than three wheels along train compartments will generate near zero influence factor R of the first dominated frequency, or this factor of the first dominated frequency is not small.

6. Summary

The moving high-speed train often produces significant ground vibrations, especially at the resonance condition, so how to avoid resonance and reduce the vibrations induced by high-speed trains has become an important issue. This paper investigates the resonant vibration characteristics of the three-dimensional vehicle–bridge system when high-speed trains pass bridges. The dominated train frequencies of nV/L can be clearly seen from the finite element analyses of the multi-span bridges with high piers and simply supported beams. To avoid resonance, the dominated train frequencies and the bridge natural frequencies should be as different as possible, especially for the first dominated train frequency and the first bridge natural frequency in each direction. If the two first frequencies are similar, the resonance can be serious.

A suitable axial stiffness between two simple beams can reduce vibrations at a near-resonance condition. The axial stiffness of the continuous railway and the friction of the bearing plate should be enough to obtain this axial stiffness. However, extra-axial links or dampers can be installed to reduce vibrations if the stiffness from the above items is not enough. This small modification of the bridge is probably the cheapest way to reduce vibrations for simple beam bridges.

Acknowledgements

This study was supported by the National Science Council, Republic of China, under contract number NSC89-2218-E-006-019.

References

[1] Y.S. Cheng, F.T.K. Au, Y.K. Cheung, D.Y. Zheng, On the separation between moving vehicles and bridge, Journal of Sound and Vibration 222 (1999) 781–801.

[2] Y.K. Cheung, F.T.K. Au, D.Y. Zheng, Y.S. Cheng, Vibration of multi-span bridges under moving vehicles and trains by using modified beam vibration functions, Journal of Sound Vibration 228 (1999) 611–628.

[3] J.Z. Li, M.B. Su, The resonant vibration for a simply supported girder bridge under high-speed trains, Journal of Sound and Vibration 224 (1999) 897–915.

[4] F.T.K. Au, J.J. Wang, Y.K. Cheung, Impact study of cable-stayed bridge under railway traffic using various models, Journal of Sound and Vibration 240 (2001) 447–465.

[5] H. Xia, Y.L. Xu, T.H.T. Chan, Dynamic interaction of long suspension bridges with running trains, Journal of Sound and Vibration 237 (2000) 263–280.

[6] Q.L. Zhang, A. Vrouwenvelder, J. Wardenier, Numerical simulation of train–bridge interactive dynamics, Computers and Structures 79 (2001) 1059–1075.

[7] Y.B. Yang, S.S. Liao, B.H. Lin, Impact formulas for vehicles moving over simple and continues beams, Journal of Structural Engineering, American Society of Civil Engineers 121 (1995) 1644–1650.
[8] Y.B. Yang, Y.S. Wu, A versatile element for analyzing vehicle–bridge interaction response, Engineering Structures 23 (2001) 452–469.
[9] S.H. Ju, Finite element analyses of wave propagations due to high-speed train across bridges, International Journal for Numerical Methods in Engineering 54 (2002) 1391–1408.
[10] S.H. Ju, T.L. Horng, Behaviors of a single crack in multiple bolted joints, International Journal of Solids and Structures 36 (1999) 4055–4070.